

## Modeling the Onset of Shallow Landslides in Partially Saturated Slopes Subjected to Rain Infiltration

J. Eichenberger, M. Sc., M. Nuth, Ph.D. and L. Laloui, Ph.D.

Laboratory of Soil Mechanics, Swiss Federal Institute of Technology Lausanne, Station 18, CH-1015, Lausanne; PH (+41) 216935398; FAX (+41) 216934153; email: john.eichenberger@epfl.ch

### ABSTRACT

Heavy rainfall can lead to shallow slips on slopes which are often initially in a state of partial water saturation. A multiphysics approach and advanced constitutive modeling are necessary to take into account the physical key processes in partially saturated soils during rainfall events, such as water flow through the solid matrix, soil water retention behavior and the effects of matric suction on the mechanical behavior. The elasto-plastic constitutive model ACMEG-s that includes an elasto-plastic water retention model with wetting-drying hysteresis is used in the framework of finite element modeling for the assessment of destabilizing, transient processes in a steep slope during rain infiltration. It is shown that at the onset of failure, wetting pore collapse and plastic shear strains occur in the lower part of the slope and develop upwards towards the slope surface to delimit a probable failure mechanism.

### INTRODUCTION

Shallow slips represent a major threat to human life and property. They are primarily triggered in partially saturated, steep slopes during stormy rainfall events. In alpine regions, the failure surface is commonly situated between 2 and 4 meters in soil depth and the whole sliding mass sums up to a couple of hundred to thousand cubic meters (Moser & Hohensinn 1983). The sliding mass develops often very high velocities (up to several m/s) leading to high impact on obstacles and sadly coming in many cases as a surprise to eyewitnesses. For the future, a higher occurrence of shallow slides is expected due to the increasing number of extreme weather events and human activities in landslide-prone areas.

Within the framework of an advanced elasto-plastic constitutive model for unsaturated soils, results from a numerical finite element analysis are presented. The considered case study is inspired from a real test-site slope in partially saturated conditions subjected to rain infiltration (Springman et al. 2009). The simulation results show the usefulness of considering partial saturation in hydraulic and mechanical terms for the modeling of the predominant transient processes and key physical mechanisms, such as soil hardening effect of matric suction, wetting pore collapse and plastic shearing.

## PHYSICAL PROCESSES IN UNSATURATED SOIL SLOPES

Commonly, two flow regimes are encountered in natural slopes: a deep flow regime, most often parallel to the slope surface with possible complex bedrock interactions and a superficial flow regime with capillary pressures or positive, compressive pore water pressures controlled by rainfall. Rain infiltration and hydrologic conditions influence the occurrence and type of triggering mechanism in landslides. The slope behavior depends mainly on the rainfall intensity and duration, on soil hydraulic characteristics, on the thickness of the sliding mass and on antecedent weather conditions (Klubertanz et al. 2009). A flow regime, parallel to the slope surface, installs itself in the upper partially saturated soil layer when the volume of infiltrated water is large enough, carrying consequently water to the toe region. Several hydromechanical processes act in a destabilizing sense on the slope. The degree of saturation of the upper soil layer increases, thereby reducing the capillary tension between the soil particles which weakens the slope. Upon that, due to the mobilized fluid flow inside the soil matrix, the fluid exerts a destabilizing, downhill frictional drag. If the rainfall intensity is higher than the capacity of the soil to dissipate the pore water, surface run-off occurs which risks to erode the slope. Depending on soil permeability and on the intensity and duration of rainfall, infiltration will lead either to shallow slides in the vadose zone, or time-delayed, deep-seated failures due to mounding of the water table (Rahardjo et al. 2007).

## THEORETICAL FRAMEWORK FOR UNSATURATED SOILS

In order to capture the main features of soil slope behavior in unsaturated conditions for modeling purpose, an elasto-plastic constitutive model including the soil water retention behavior is used in the framework of hydromechanically coupled porous media. The principal model concepts are reviewed in this section.

The Advanced Constitutive Model for Environmental Geomechanics (ACMEG-s) (Nuth & Laloui 2007; Nuth & Laloui 2008a) is a Cam-Clay-type elasto-plastic model (Schofield & Wroth 1968) and is based on the so-called initial Hujieux's model (Hujieux 1979). The increment of strain  $d\varepsilon_{ij}$  is decomposed into:

$$d\varepsilon_{ij} = d\varepsilon_{ij}^e + d\varepsilon_{ij}^p$$

where  $d\varepsilon_{ij}^e$  is the elastic strain increment and  $d\varepsilon_{ij}^p$  the plastic strain increment.

The elastic deformation can be expressed as:

$$d\varepsilon_{ij}^e = C_{ijkl} d\sigma'_{kl} \quad (1)$$

The tensor  $C_{ijkl}$  is the mechanical elastic tensor and is composed of non-linear elastic moduli. The elastic strain increment  $d\varepsilon_{ij}^e$  can be decomposed in volumetric

and deviatoric increments which are related to mean effective, respectively deviatoric stress by means of spherical stress-dependent elastic moduli.  $\sigma'_{kl}$  in equation (1) is the effective stress for unsaturated soils:

$$\sigma'_{kl} = (\sigma_{kl} - u_a \delta_{kl}) + S_r (u_a - u_w) \delta_{kl} \quad (2)$$

where  $\sigma_{kl}$  is the total stress,  $u_a$  is the air pressure,  $u_w$  is the water pressure,  $S_r$  is the degree of saturation and  $\delta_{kl}$  is the Kronecker's delta ( $\delta_{kl} = 1$  if  $k = l, 0$  else). The difference between the total stress  $\sigma_{kl}$  and the air pressure  $u_a$  is called the net stress  $\sigma_{klnet}$ . The difference between  $u_a$  and  $u_w$  is defined as the matric suction  $s$ .

The critical state line is defined in the plane of deviatoric stress  $q$  versus mean effective stress  $p'$ , with a slope  $M$ . The slope of the critical state line in the plane volumetric plastic strain vs. mean effective stress ( $\varepsilon_v^p - \ln p'$ ) is  $\beta$ ,  $p'_{CR0}$  being the initial critical state pressure:

$$\ln \frac{p'_{CR}}{p'_{CR0}} = \beta \varepsilon_v^p \quad (3)$$

In the ACMEG-s model, the plastic irreversible strain increment  $d\varepsilon_{ij}^p$  is induced by two coupled dissipative processes: an isotropic and a deviatoric plastic mechanism. The yield limits of each mechanism, bounding the elastic domain in the effective stress space, can be written as:

$$\tilde{f}_{iso}(p', \varepsilon_v^p, r_{iso}) = p' - r_{iso} \cdot d \cdot p'_{CR} \quad (4)$$

$$\tilde{f}_{dev}(p', q, r_{dev}, \varepsilon_v^p, \varepsilon_d^p) = q - Mp' \left( 1 - b \ln \frac{p'}{p'_{CR}} \right) r_{dev} \quad (5)$$

where  $p'_{CR}$  is the critical state pressure.  $d$ ,  $b$ ,  $r_{iso}$  and  $r_{dev}$  are material parameters.  $\varepsilon_v^p$  and  $\varepsilon_d^p$  are respectively the volumetric plastic strain and the deviatoric plastic strain. The critical state pressure in equation (3) can be related to the preconsolidation pressure  $p'_c$  using the material parameter  $d$ , that represents the distance in the volumetric plane between the normally consolidated line and the critical state line:

$$p'_c = d \cdot p'_{CR}$$

Using the space of triaxial stress variables  $q$  and  $p'$ , the elastic domain is enclosed by an ellipsoidal surface which is cut by the isotropic yield limit (see Figure 1). Adding the suction  $s$  as a third axis of the space, Figure 1 shows that the elastic domain gets larger with suction. This accounts for the fact that a dryer material will

have higher strength and stiffness. The equation (6) gives the mathematical formulation of the contribution of the capillary effects to the mechanical behavior. The principle is to introduce a dependency of the preconsolidation pressure  $p'_c$  on the level of suction  $s$  and using a material parameter  $\gamma_s$  :

$$p'_c = \begin{cases} p'_{c0} & \text{if } s \leq s_e \\ p'_{c0} [1 + \gamma_s \log(s/s_e)] & \text{if } s \geq s_e \end{cases} \quad (6)$$

$p'_{c0}$  is the initial preconsolidation pressure at zero suction and  $s_e$  is the suction air entry.

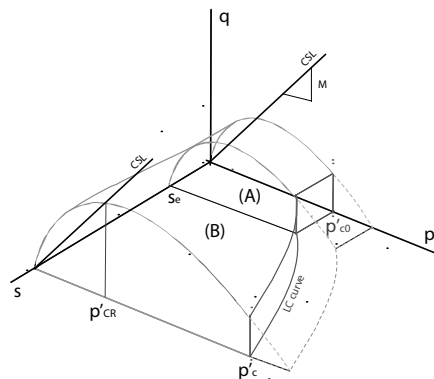


**Figure 1. Yield surface shape and critical state line (CSL) in a  $(p', q, s)$  space.**

Modeling the evolution of the degree of saturation  $S_r$  with respect to suction  $s$  is also taken into account in the model (Nuth & Laloui 2008b). The increment of the degree of saturation  $dS_r$  is decomposed into an elastic part and a plastic part and is written:

$$dS_r = \frac{ds}{K_H \times (s/s_e)} + \frac{ds_D}{\beta_H \times (s_D/s_{D0})}$$

$K_H$  is the elastic slope and  $\beta_H$  is the plastic slope defined in Figure 2.  $s_e$  represents the limit below which the degree of saturation remains equal to one.  $s_e$  depends on the void ratio (i.e. the density of the material). If the suction remains lower than the air entry value, the degree of saturation equals one and there is no elastic increment. If the residual state is reached ( $S_r = S_{res}$ , where  $S_{res}$  is the residual degree of saturation), then the elastic increment becomes null too.  $s_D$  is the drying yield suction, which is the maximum suction ever experienced by the material along a drying path.  $s_{D0}$  is the initial value of the drying yield suction.

The process of drying and wetting is not fully reversible and the  $(S_r - s)$  data usually show the existence of a capillary hysteresis. A given level of suction can indeed correspond to different degrees of saturation. The way chosen to reproduce the retention hysteresis is to make the yield surface evolves by means of kinematic hardening. The elastic domain is delimited by the following yield limit:

$$f = \left\| \ln(s) - \ln(s_D) + \frac{1}{2} [\ln(s_{D0}) - \ln(s_e)] \right\| - \frac{1}{2} [\ln(s_{D0}) - \ln(s_e)]$$

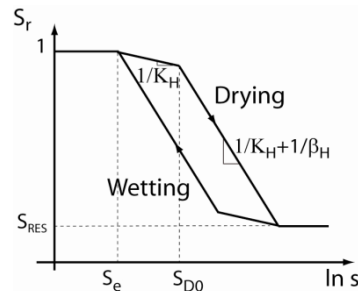


**Figure 2. Modeling of the soil water retention curve.**

For the flow problem, the generalized Darcy's law is used to describe the relative velocity of the fluid with respect to the solid skeleton. The permeability tensor  $\mathbf{K}_w$  depends in general on the degree of saturation  $S_r$ . Assuming hydraulic isotropic conditions, the water relative permeability coefficient  $k_{rw}$  is defined according to the following relationship, CKW1 being a material parameter:

$$k_{rw} = \sqrt{S_r} \left[ 1 - \left( 1 - S_r^{\frac{1}{CKW1}} \right)^2 \right]$$

The constitutive model presented above is implemented into the finite element code called LAGAMINE (Charlier 1987; Collin 2003). The code features hydro-mechanically coupled finite elements.

## NUMERICAL MODELING OF AN UNSATURATED SOIL SLOPE SUBJECTED TO A RAINFALL EVENT

As a generic case study, the hydromechanically coupled analysis is inspired from realistic geometrical (Askarinejad 2009) and material parameters (Eyraud 2009) close to those of a real test-site case study in Rüdlingen, Switzerland (Swiss Competence Center Environment and Sustainability, project TRAMM). A detailed description of this landslide triggering experiment is presented by Springman et al. (2009). It is not intended here to reproduce the in-situ experiment neither to compare the performance of the model with the measured in-situ data. The material parameters for the ACMEG-s model were calibrated on the basis of triaxial, oedometer and retention tests carried out at the Laboratory of Soil Mechanics, EPFL (Table 1). The

geometry of the slope is presented in Figure 3. The steep slope of  $38^\circ$  is composed of silty sand deposits (soil cover) of 2 to 5m thickness and a beneath laying bedrock. The principal objective of this study is to show the effect of rain infiltration on the stability of a partially saturated slope and its failure mechanisms.

### Definition of the Geomechanical Model and the Calculation Procedure

The finite element mesh presented in Figure 3 is composed of 4672 six-noded quadratic triangles. The ACMEG-s constitutive model is applied to both, bedrock and soil cover, using the parameters of table 1. The behavior of the bedrock is assumed elastic. The mesh is strongly refined in the upper soil layer in order to properly model the transient hydromechanical processes and the development of plastic zones during rain infiltration. Conventional kinematic boundary conditions are imposed to the box model.

**Table 1. Parameters for the elasto-plastic ACMEG-s and water retention model.**

		<i>Symbol</i>	<i>Description</i>	<i>Value</i>
Stress-strain model	Elastic parameters	$K_{ref}$	Bulk modulus	$1 \cdot 10^9$ Pa
		$G_{ref}$	Shear modulus	$6 \cdot 10^8$ Pa
		$n^e$	Elastic exponent	0.1
	Plastic parameters	$\varphi'$	Friction angle	$33^\circ$
		$\beta_0$	Compressibility coefficient	30
		$*\alpha$	Dilatancy coefficient	0.7
		$*a$		0.05
		$b$	see equation (5)	0.1
		$*c$		0.08
	Limits of elastic domain	$d$	see equation (4)	1.3
$\Gamma_{dev}^e$		Initialisation of deviatoric mechanism	0.3	
Capillary effects	$\Gamma_{iso}^e$	Initialisation of isotropic mechanism	0.3	
	$\gamma_s$	Coefficient of LC curve	0.78173	
	$*\Omega$	Coef. var. compressibility	$2 \cdot 10^{-5}$	
Retention model	$S_e$	Air entry value	3000 Pa	
	$K_h$	Elastic coefficient	8.8	
	$\beta_h$	Plastic coefficient	10	
	$S_{D0}$	Drying yield suction	6000 Pa	
Permeability	$S_{res}$	Residual degree of saturation	0.3	
	$k_{w,sat}$	Intr. water permeability	$10^{-5}$ m/s	
	CKW1	Parameter for the water rel. perm. function	0.123	

\*see Nuth & Laloui 2007 for explanation of parameters.

Initially, two calculations are run which consist of a gravity loading phase and a coupled flow and deformation analysis for the determination of the water table position and distribution of matric suction in the vadose zone. The resulting water table runs inclined from the top left to the bottom right model boundary. Matric

suction is distributed hydrostatically in the partially saturated zone above the water table and the degree of saturation reaches its residual value of  $S_r = 0.3$  along the slope surface, see Figure 3.

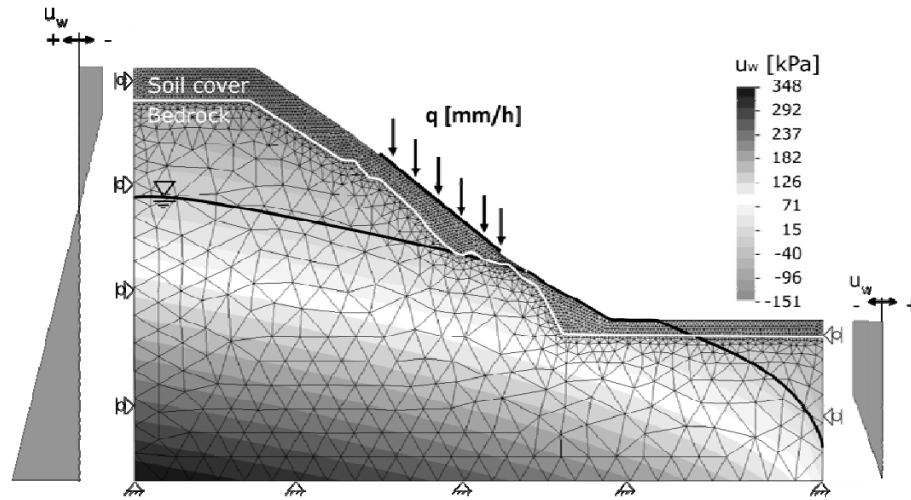


**Figure 3. Finite element mesh, boundary and initial conditions**

In a final step, rain infiltration is simulated by means of an imposed boundary flux of 15mm/h for 3.5 days (the rain input is virtual and does not correspond to the real experiment). The water saturation contours in Figure 4a show clearly that the superficial soil layer has been quasi completely saturated. The soil water retention curve in Figure 4b indicates for 3 points at different depths that the matric suction has decreased to reach zero or close to zero values.

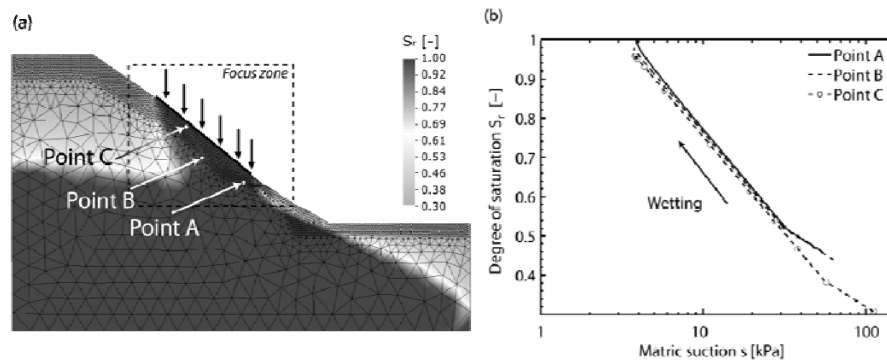


**Figure 4. Rain infiltration in a partially saturated slope: spatial distribution of the degree of saturation (a); Soil water retention curve (b)**

**Plastic Mechanisms during Rain Infiltration**

The supply of water in a partially saturated slope acts negatively on its stability. With increasing water content, the capillary forces reigning between the soil particles decrease. This de-bonding effect of wetting is taken into account in the model through the effective stress (Eq. (2)), which decreases during rain infiltration. The soil loses strength in classical soil mechanics terms.

In Figure 5, the contours of deviatoric strains are shown for the "focus zone" indicated in Figure 4. Shear strains are localized along the interface between bedrock and soil layer for the lower and middle part of the slope and run up biased to the slope surface in the upper part. The extent of the shear zone coincides with the zone of increased degree of saturation (Figure 4a), showing clearly a localized effect of the infiltrated water.

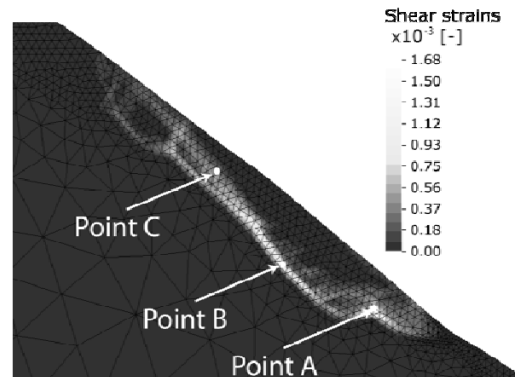


**Figure 5. Contour of deviatoric strains after 3.5 days of rain infiltration. Light zones indicate a concentration of shear strains.**

The deformation history of three selected points A, B and C defined in Figure 5 indicate which plastic mechanism, among the isotropic (Eq. (4)) and deviatoric (Eq. (5)), is predominant in different parts of the slope at different instants in time. The soil in the vicinity of point A above the bedrock abutment was almost normally consolidated prior to infiltration. In this zone, water infiltration is at the origin of strong shearing associated with noticeable positive (compressive) plastic volumetric deformations (Figure 6).

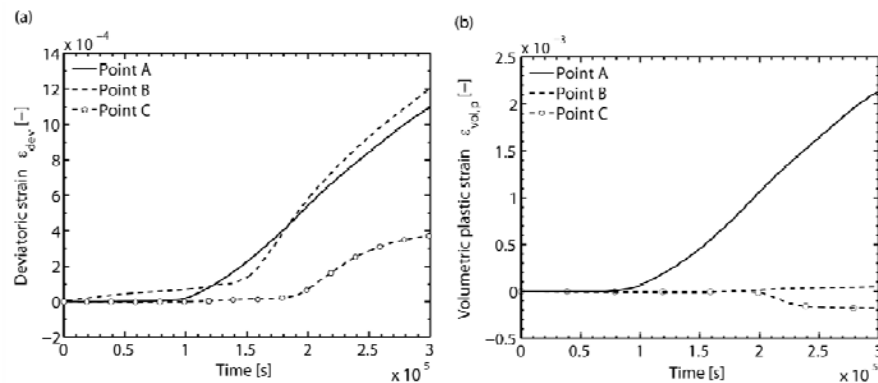


**Figure 6. Evolution of deviatoric (a) and plastic volumetric (b) deformations**

Compared to the other observation points, the volumetric behavior in point A is clearly distinguished. Point B situated in the middle part of the slope undergoes strong shearing of the same order of magnitude as for point A. The compressive plastic volumetric deformation at point B is however negligible. Point C located in the shearing zone running up to the slope surface reacts only after  $2 \times 10^5$  seconds. In

accordance with the other observation points this suggests that the shearing mechanism starts in the lower part of the slope, above the abutment, then moves upwards along the bedrock interface and finally runs up to the slope surface, delimiting consequently a potentially unstable soil mass. The plastic volumetric strains in point C are negative in the sense of extension and are associated to the occurrence of plastic deviatoric strains. The extension of the soil can be either due to dilatancy during shearing, considering that the soil is overconsolidated, or due to a downwards movement of the potentially unstable soil mass leading to the formation of a tension crack in the upper part of the slope.

The almost normally consolidated soil in the lower part of the slope is a priori susceptible to plastic deformations in the sense of a wetting pore collapse. The wetting pore collapse is the property of the soils to get denser when soaked under a sufficient mechanical load. As shown in Figure 7a for points A and B the stress paths during wetting remain at first within their respective elastic domains. The isotropic yield limits are reached at lower values of matric suction. The stress paths then follow the current isotropic yield surfaces without moving them noticeably. Yet, this process corresponds to soil hardening and generation of compressive volumetric plastic strains. This behavior was experimentally observed in confined testing conditions and is coherent with the simulated conditions in the soil slope. There is a considerable loss in mean effective stress associated to the wetting pore collapse in point A after  $7 \cdot 10^4$  seconds which indicates a strength decrease in the lower part of the slope (Figure 7b). The mean effective stress reaches a constant value of around 60kPa after  $1.5 \cdot 10^5$  seconds. Matric suction decreases to a steady constant value of around 5kPa.

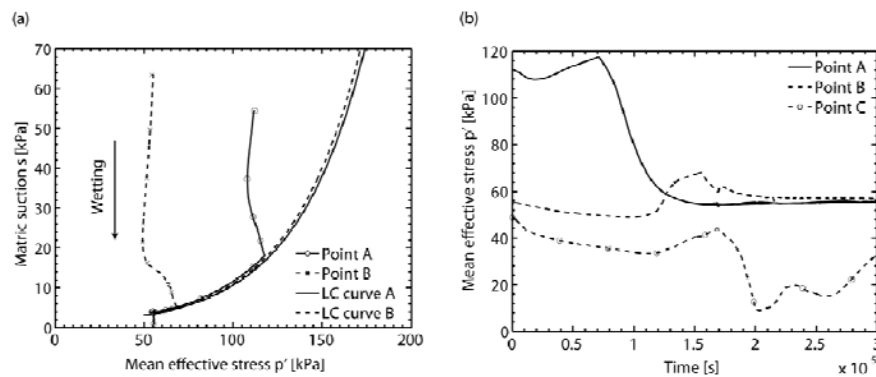


**Figure 7. Stress paths and loading collapse curves (isotropic yield loci) for two points (a); Evolution of mean effective stresses (b)**

To summarize, the deviatoric plastic mechanism is clearly predominant in the upper and middle part of the slope while in the lower part of the slope the isotropic plastic mechanism governs the behavior.

## CONCLUSIONS

A consistent stress framework is an essential prerequisite for the constitutive modeling of unsaturated soils. The material behavior depends on the interaction between the mechanical stress-strain response and the water retention aspect. A

hydromechanically coupled, transient finite element analysis of a partially saturated slope subjected to rain infiltration revealed the actual onset of failure. Due to adequate constitutive modeling, the model is capable of giving detailed information on the active physical mechanisms during rain infiltration. The most probable failure mechanism develops in the lower part of the slope as a consequence of a wetting pore collapse and then spreads upwards along the bedrock and through the soil cover to the slope surface as a predominant shear mechanism.

## ACKNOWLEDGEMENTS

This work was supported by Swiss Competence Center Environment and Sustainability, TRAMM project and the European Commission, FP7 project SafeLand.

## REFERENCES

- Askarinejad, A. (2009). "A method to locate the slip surface and measuring subsurface deformations in slopes." *Proc. 4th Intern. Young Geotechnical Engineers' Conf.*, Alexandria, Egypt: 171-174.
- Charlier, R. (1987). Approche unifiée de quelques problèmes non linéaires de mécanique des milieux continus par la méthode des éléments finis. *PhD thesis*, Université de Liège.
- Collin, F. (2003). Couplages thermo-hydro-mécaniques dans les sols et les roches tendres partiellement saturés. *PhD thesis*, Université de Liège.
- Eyraud, N. (2009). Experimental Characterisation of a Clayey Sand for Unsaturated Model Calibration. Internship report, EPFL, Lausanne: 64p.
- Hujeux, J. (1979). Calcul numérique de problèmes de consolidation élastoplastique. *PhD thesis*, Ecole Centrale Paris.
- Klubertanz, G., Laloui, L., Vulliet L. (2009). "Identification of mechanisms for landslide type initiation of debris flows." *Engineering Geology*. 109 (1-2): 114-123.
- Moser, M., Hohensinn, F. (1983). "Geotechnical aspects of soil slips in alpine regions." *Engineering Geology*. 19: 185 – 211.
- Nuth, M., Laloui, L. (2007). "New insight into the unified hydro-mechanical constitutive modeling of unsaturated soils." *Proc. Unsat Asia 2007*. Nanjing: 109-125.
- Nuth, M., Laloui, L. (2008a). "Effective stress concept in unsaturated soils: Clarification and validation of a unified framework." *International journal for numerical and analytical methods in Geomechanics*. 32: 771-801.

- Nuth, M., Laloui L. (2008b). "Advances in modeling hysteretic water retention curve in deformable soils." *Computers and Geotechnics*. 35 (6): 835-844.
- Rahardjo, H., Ong, T.H., Rezaur, R.B., Leong, E.C. (2007). "Factors controlling instability of homogeneous soil slopes under rainfall." *Journal of Geotechnical and Geoenvironmental Engineering*. 133(12): 1532-1543.
- Schofield, A.N., Wroth, C.P. (1968). *Critical state soil mechanics*, McGraw-Hill, London.
- Springman, S.M., Kienzler, P., Casini, F., Askarinejad, A. (2009). "Landslide triggering experiment in a steep forested slope in Switzerland." *17th Intern. Conf. of Soil Mech. & Geot. Eng.*, Alexandria, Egypt: 1698 - 1701.